Effects of fiber gripping methods on the single fiber tensile test: I. Non-parametric statistical analysis

Jae Hyun Kim · N. Alan Heckert · Stefan D. Leigh ·
Haruki Kobayashi · Walter G. McDonough ·
Kirk D. Rice · Gale A. Holmes

Abstract Single fiber tensile tests using two different gripping methods were carried out on various fiber lengths. One method (the glue-tab grip method) consists of mounting a fiber onto a rigid tab as specified in ASTM C1557-03 using an adhesive, while the other (the direct grip method) involves directly clamping a fiber using poly(methyl methacrylate) blocks. The tensile moduli obtained by the glue-tab grip as a function of the fiber gauge length are clearly different from those of the direct grip for fiber length between 2 and 10 mm, based on graphical statistical analyses using kernel density and q–q plots. This difference is caused by the gripping effect. In addition, the tensile strains and strengths obtained by the glue-tab grip were different from those of the direct grip at the short fiber gauge lengths (i.e., 2–10 mm). The differences between the tensile properties (i.e., modulus, strain, and strength) for the two grips measured with the 60-mm fiber length were not statistically significant compared to the results with the short fiber lengths.

J. H. Kim · H. Kobayashi · W. G. McDonough (✉) ·
G. A. Holmes
Polymers Division (M/S 8541), National Institute of Standards
and Technology, Gaithersburg, MD 20899, USA
e-mail: walter.mcdonough@nist.gov

N. A. Heckert · S. D. Leigh
Statistical Engineering Division (M/S 8980), National Institute
of Standards and Technology, Gaithersburg, MD 20899, USA

Present Address:
H. Kobayashi
Department of Macromolecular Science and Engineering,
Graduate School of Science and Technology, Kyoto Institute
of Technology, Matsugasaki, Kyoto 606-8585, Japan

K. D. Rice
Office of Law Enforcement Standards (M/S 8102),
National Institute of Standards and Technology,
Gaithersburg, MD 20899, USA

Introduction

To enhance the protection and comfort levels of a first responder, lightweight soft body armor (SBA) requires further improvements to fibers, ballistic properties, and long-term durability under various environmental conditions. Factors influencing the ballistic performance of SBA include mechanical properties of fibers and yarns (e.g., modulus, strain-to-failure, ultimate tensile strength) and interactions of neighboring fibers or layers [1]. Ballistic parameters for SBA fibers and yarns are usually characterized under slow test speed conditions, although designing SBA clearly requires that material properties be measured at a ballistic test speed. The lack of reliable fiber properties' data measured at ballistic impact speeds continues to hinder the development of certification protocols to insure the reliability of SBAs over their projected lifespan. The importance of obtaining accurate and reproducible high strain rate (HSR) test data on these fibers to insure their ballistic performance in lightweight SBA applications was underscored in two recent workshops [2, 3].

Recent developments in HSR testing methodologies using the Split Hopkinson Bar (SHB) for yarns and fibers have sought to overcome this deficiency in test speeds [4, 5]. However, since HSR tests using the SHB typically require short specimen gauge lengths, this requirement coupled with the HSR test condition can be problematic for extracting meaningful fiber properties' data. For instance, the 2-mm fiber used in the HSR research has an aspect ratio of approximately 133–200 [4]. However, until 1998, the recommended minimum aspect ratio under ASTM D3379-75

[6] for the static testing of a single fiber was 2000, chosen to minimize the tested gauge length perturbed by the gripping area. ASTM D3379-75 was superseded by ASTM C1557-03, in part because of the technical inaccuracies associated with the use of the average of the cross-sectional area of several fibers for the calculation of individual fiber strengths. ASTM C1557-03 allows testing of shorter lengths, so long as the gauge length is reported [7]. Implicit in this protocol change is the assumption that the perturbed stress fields in the gripping regions are constant in the standard testing configuration. However, a common problem experienced in the preparation of single fiber test samples with shorter gauge lengths is wicking of glue along the fiber length that effectively seals flaws on the fiber surface and enhances fiber strength [8], so that the effective gauge length becomes much shorter and essentially unknown.

To successfully conduct single fiber tests under HSR, it is important to recognize that the perturbed stress field may exert more influence due to a relatively shorter gauge length compared to a conventional single fiber test under slow test speed conditions. In this study, a systematic investigation using fibers with various gauge lengths is undertaken to compare the statistics of fiber strengths. Since we focus on developing a test method, PPTA fibers that show more stable mechanical properties than another high strength fiber such as PBO [9] are used as test specimens. The two different fiber gripping methods are introduced: directly gripping a single fiber (direct gripping) versus adhering a fiber onto a stiff tab for clamping (glue-tab gripping). The glue-tab method is currently being used in HSR testing. However, the methodology is time consuming, limiting the experiments to a few tests per day. Given that fiber strength is stochastic, sample sizes sufficient to yield statistically significant results are necessary to truly determine fiber properties. It is worth noting that research employing the direct gripping method has been mainly utilized to conduct rapid assessment of single fiber properties such as tensile strength, modulus, and ultimate strain with a higher aspect ratio than 2000 [10]. Although the ultimate goal is the assessment of ballistic fiber properties under HSR conditions, this initial study focuses on test data taken under static test conditions using glue-tab and direct fiber gripping methods. In addition, since the fiber gauge length for HSR conditions is a few millimeters, we focus on the test data obtained by short fiber lengths.

Experimental

Fiber gripping methods

Poly(*p*-phenylene terephthalamide) fibers (PPTA) and two types of fiber gripping techniques are used in this study.

The specimens for which a single fiber was glued (i.e., the glue-tab grip method) onto a rigid tab as shown in Fig. 1a were prepared based on ASTM C1577-03. A brief description of the procedure for preparing single fiber tensile test specimens using the glue-tab grip is as follows: Individual fibers for the 2-mm gauge length test are temporarily attached to thin plastic sheet templates having more rigid surface than paper. Paper sheet templates were used for the 5-, 10-, and 60-mm length tests. The grid lines of all dimensions for templates were printed by a laser printer. The fiber is fixed to the template using a cyanoacrylate-based adhesive which appears to bond better to the fiber than an epoxy-based adhesive. The single fiber specimens with adhesives are cured at room temperature for at least 48 h before the test. The length of the fiber embedded into the adhesive is approximately 15 mm and the length of the jaw face of the metal clamp is 12 mm. An alternative approach is to directly grip a single fiber using the mechanical grips as shown in Fig. 1b. A single PPTA fiber is clamped directly between two poly(methyl methacrylate) blocks at both ends and the clamping force of the blocks is controlled by tightening a spring. Compared to the glue-tab grip, the direct grip reduces the sample preparation time since adhesives are not used. Fiber diameters for both gripping methods were measured on an optical microscope at five equally spaced locations for each fiber, and an average of the five measurements was used for calculating a fiber cross section.

Tensile tests were carried out under a constant strain rate 0.00056 s^{-1} for all gauge lengths. The loading device for
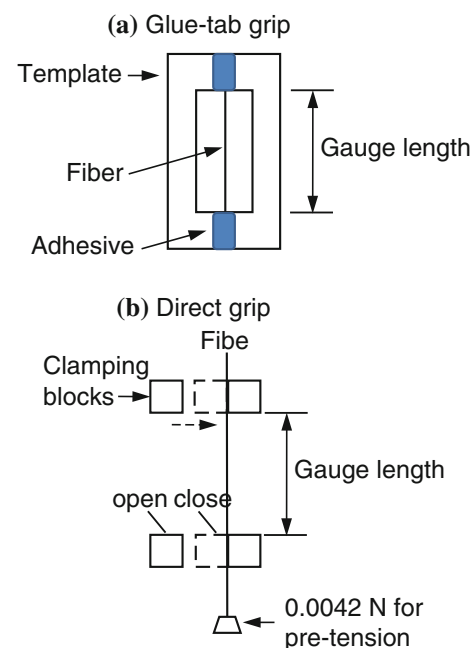
Fig. 1 Schematic and close up of the mechanical grips for single fiber tensile loading

the glue-tab grip is an electromagnet actuator and for the direct grip, it is a screw-driven machine. Both actuating systems appear to be no different with respect to tolerance of movement. Single fiber strength was calculated from the load at fiber failure and the cross section calculated from the average diameter determination. Standard deviations in the load cell as a standard uncertainty for both loading devices are less than 1 %.

Graphical methods for statistical analysis

In this study, two statistical analysis methods are applied to differentiate between sets of measurements graphically. The quantile–quantile (q–q) plot is a graphical technique for determining if two datasets come from a common distribution. It plots the quantiles of the first dataset against the corresponding quantiles of the second dataset. A quantile of a distribution is the point below which a given fraction (or percent) of points lies. For example, a 30 % quantile of a distribution is the point at which 30 % of the data falls below and 70 % falls above. If the two sets are well represented by the same distribution, these points should fall approximately along a 45-degree reference line (slope = 1, intercept = 0). This reference line is shown on the plot with the correlation coefficient (CC), slope (A1) and intercept (A0) of the fitted line for the points. The greater the departure from this reference line, the greater the evidence for the conclusion that the two datasets have come from distinct underlying populations with different distributions [11, 12].

The kernel estimate of a density f based on a set of data points is defined as

$$f_h(x) = \frac{1}{nh} \sum_{j=1}^{n} \frac{K(x - x_j)}{h} \qquad (1)$$

where K is a weighting function, h is a window width, and n is the number of data points.

That is, at any given point x (i.e., single datum), the local density is estimated as a weighted sum of the points in the data window, with weights typically based on the distance of the x_j from x. A histogram is a simple kernel density estimate computed at the midpoints of the bins, with fixed bin width h, and K a boxcar function, (i.e., points in the bin are given a weight of 1 and points outside the bin are given a weight of 0). The kernel density plots in this paper were constructed using Algorithm 176 from Applied Statistics [13]. This algorithm uses a Gaussian weighting function with $h = \frac{0.9 \mathrm{Min}(s, I_Q)}{\sqrt[5]{n}}$, where the range of the middle 50 % of the data s is standard deviation and n is the sample size. I_Q denotes the inter-quartile range (the difference between the 75th and 25th percentile of the data).

Results and discussion

Stress–Strain behaviors, failure strains, and ultimate strengths of fibers measured by the glue-tab and direct grips.

Stress–strain curves using the glue-tab and direct grip methods for gauge lengths of 2, 5, 10, and 60 mm are shown in Fig. 2a–h. We only show a few curves for each condition to allow the reader to see the variation in stress and strain values as well as differences in the shape of the stress–strain curves. The stress–strain curves for the glue-tab grip test tend to show non-linear behavior starting around 2 % strain, particularly for the smaller gauge lengths (i.e., 2–10 mm), compared to the direct grip test. In addition, repeatability shown in the stress–strain curves obtained by the glue-tab grip is somewhat poorer than in the direct grip test. The potential cause of the non-linearity for the glue-tab grip at 2-mm gauge length may be complex stress conditions in the vicinity of the gripping area during loading due to adhesive wicking [14], but the cause of the non-linearity for the direct grip at 2 mm should be different due to its direct fiber gripping mechanism. To estimate the perturbed length of the fiber within the gauge length, the St. Venant's principle can be applied. It basically asserts that the stress field exerted in an isotropic material from an external load is uniform over some distance from the points of application. This stress decay length was taken as one lateral dimension for the isotropic material. However, the perturbed distance for anisotropic materials is longer and the decay length for circular cylinders is given by [15, 16]

$$\delta = R \left(\frac{E}{E_t} \right)^{1/2} \qquad (2)$$

where R is the radius of the cylinder, and E and E_t are the longitudinal and transverse Young's moduli of the cylinder, respectively. Approximating a cylindrical fiber cross section, Eq. (2) provides a minimum allowable gauge length. The perturbed length (2δ) for PPTA fibers is approximately 0.13 mm, assuming $E = 80$ GPa, $E_t = 0.77$ GPa, and $R = 0.013$ mm as the PPTA fiber properties, which is a 7 % perturbed length for the 2-mm gauge length, but reduces to 0.2 % for the 60-mm gauge length. Although the decay lengths of the fiber obtained for the glue-tab and direct grip methods may be different due to different gripping mechanisms, it is clear that the decay lengths decrease with increasing the gauge length (e.g., 3–1 % as the gauge length increases from 5- to 10-mm length), so the gripping effects are less significant.

Figure 3 shows the corrected tensile modulus measured by the glue-tab and direct grip tests. The corrected modulus is given by
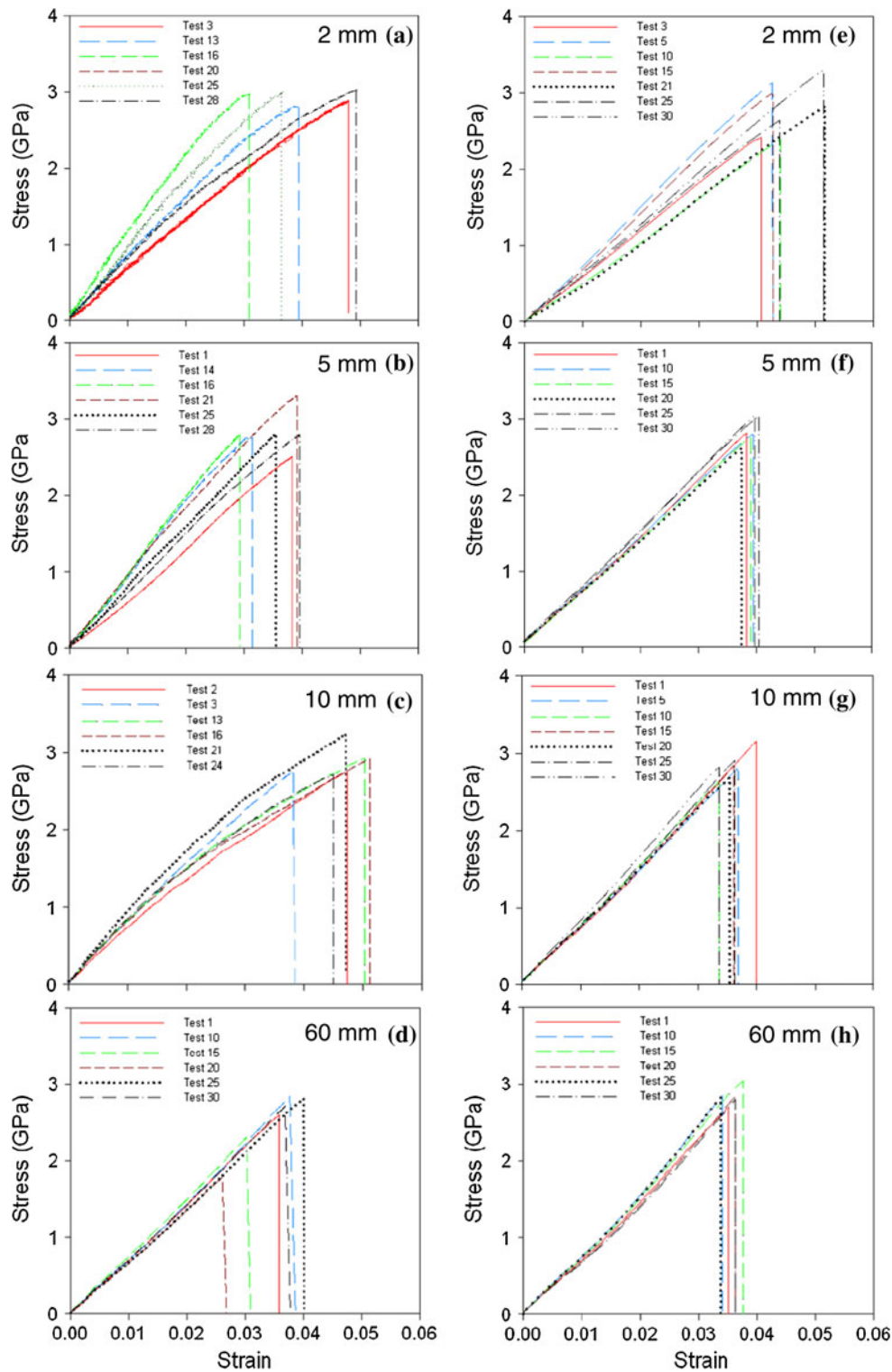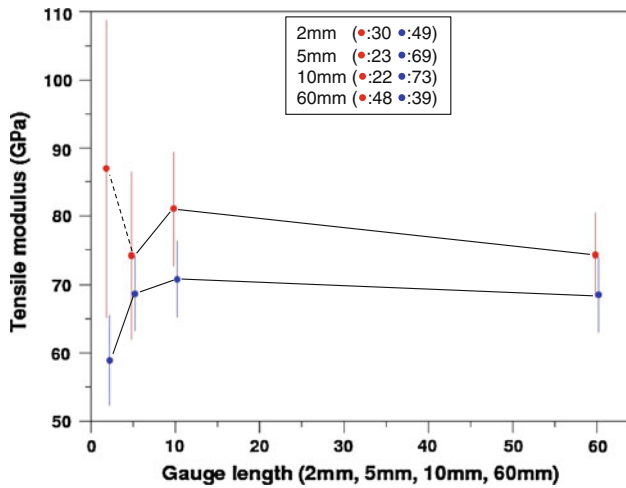
Fig. 2 Stress-strain *curves* using the glue-tab and direct grip methods for gauge lengths of 2, 5, 10, and 60 mm

$$E_{corrected} = \frac{L_0}{A(C_a - C_s)} \quad (3)$$

where C_a is the apparent compliance which is the inverse of the slope of the initial linear region of the load versus

displacement curve, C_s is the system compliance, and L_0 is the fiber gauge length having a cross-sectional area (A).

The trend of the average tensile moduli obtained by the glue-tab grip is not consistent within experimental

Fig. 3 Tensile modulus measured by the glue-tab (*red*) and direct grips (*blue*) at the various gauge lengths from 2 to 60 mm. The error bar indicates one standard deviation. The numbers of specimens are shown with symbols and the symbols at each gauge length are offset for clarity (Color figure online)
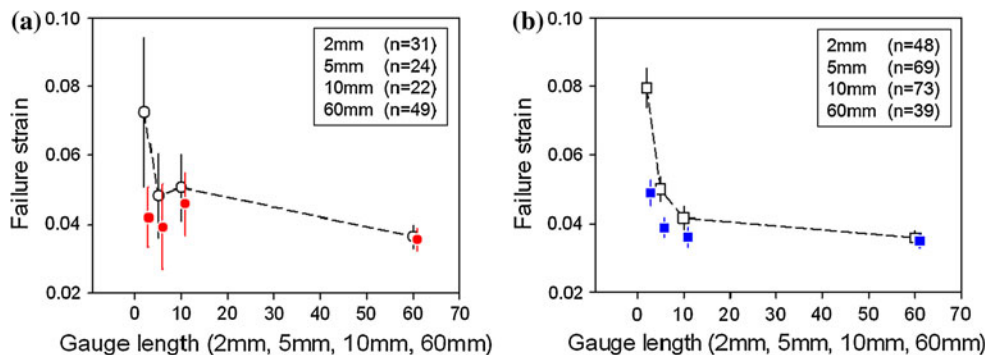
whole. Moreover, adhesive wicking on the fiber surface at the short fiber length for the glue-tab grip could contribute to cause a more complex load distribution in vicinity of the grip. These combined effects in the glue-tab are thought to result in highly scattered tensile modulus values at the 2-mm gauge length, while only the end effect contributes to the case of the direct grip test.

Figure 4 shows the corrected failure strains measured by the glue-tab and direct grip tests using gauge lengths from 2 to 60 mm. Since the strain-to-failure was not measured directly from the fiber itself but from the crosshead displacement, system compliances of the tensile tests were determined in order to correct failure strain based on the ASTM test procedure. The system compliances (C_s) determined experimentally were 0.122 (mm/N) $\pm$ 0.035 (mm/N) for the glue-tab grip test and 0.143 (mm/N) $\pm$ 0.018 (mm/N) for the direct grip test. The corrected failure strain is given by

$$\varepsilon_{corrected} = \frac{\Delta L - C_s F}{L_0} \tag{4}$$

where ΔL is the crosshead displacement measured from the test and F is the force at failure.

The failure strains for both tests are considerably reduced, particularly at the shorter gauge lengths (i.e., 2–5 mm), by correcting for system compliance. The failure strains of the glue-tab grip tests show relatively bigger variations at the shorter gauge lengths from 2 to 10 mm compared to the direct grip tests, which is similar to the trend of the modulus. In addition, the average failure strains measured by the glue-tab grip vary erratically with increasing gauge length within experimental uncertainty, while the average failure strains obtained by the direct grip tests decrease consistently with increasing gauge length. The variation of failure strains at 60-mm gauge length is relatively small for both grips. Since a fiber has a lower probability of containing flaws at the shorter fiber lengths [18], the fiber failure strain is increased at shorter fiber

uncertainty when compared to the results of the direct grip test, but shows relatively higher variation over the short fiber lengths (i.e., from 2 to 10 mm), particularly at 2 mm. The average modulus for the direct grip test initially increases with the fiber gauge length from 2 mm to 5 mm and then shows a plateau from 10 to 60 mm. The change of the average modulus values for both grips becomes relatively smaller as the gauge length increases from 10 to 60 mm. This trend, showing increasing modulus at the short fiber gauge lengths, but then becoming constant over the longer gauge length range, has been previously reported for highly oriented polymers [17].

Since tensile load in the vicinity of the clamp is perturbed by the end effect, a relatively higher fraction of the fiber length is subject to the end effect for any short fiber gauge length, which can produce a larger fiber strain, and so underestimates the true tensile modulus for the fiber as a

Fig. 4 Uncorrected (open symbols) and corrected (*filled*) failure strains measured by the glue-tab (**a**) and direct grips (**b**) at the various gauge lengths from 2 to 60 mm. The error bar indicates one standard deviation. The numbers of specimens are shown with symbols and the symbols at each gauge length are offset for clarity
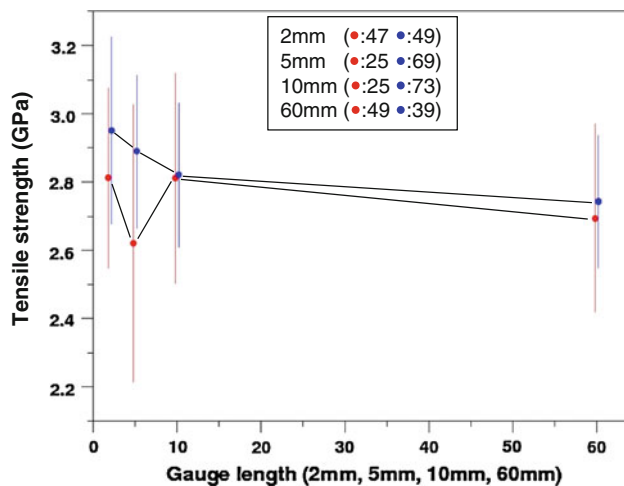
Fig. 5 Tensile strengths measured by the glue-tab (*red*) and direct grips (*blue*) at the various gauge lengths from 2 to 60 mm. The error bar indicates one standard deviation. The numbers of specimens are shown with symbols and the symbols at each gauge length are offset for clarity (Color figure online)

lengths. As the fiber length increases, the probability of containing a flaw is increased, so the fiber failure strain is decreased before it becomes almost constant eventually over a long fiber gauge length, i.e., at 60 mm. This behavior of the fiber failure strain with gauge length agrees better with the results of the direct grip.

Figure 5 shows the tensile strengths measured by the glue-tab and direct grips for gauge lengths 2–60 mm. Although several specimens measured by the glue-tab grip showed a highly non-linear behavior and were discarded from the analysis of the modulus and failure strain, these discarded samples were included in the strength analysis, but the trend between the strength and gauge length for the glue-tab grip test was not changed whether these data were included or not. Although both tests show similar results compared with the results of failure strains, the trend of average tensile strengths for the glue-tab grip tests is not consistent within experimental uncertainty, while the direct grip tests show the consistent trend of the average strengths over the fiber lengths.

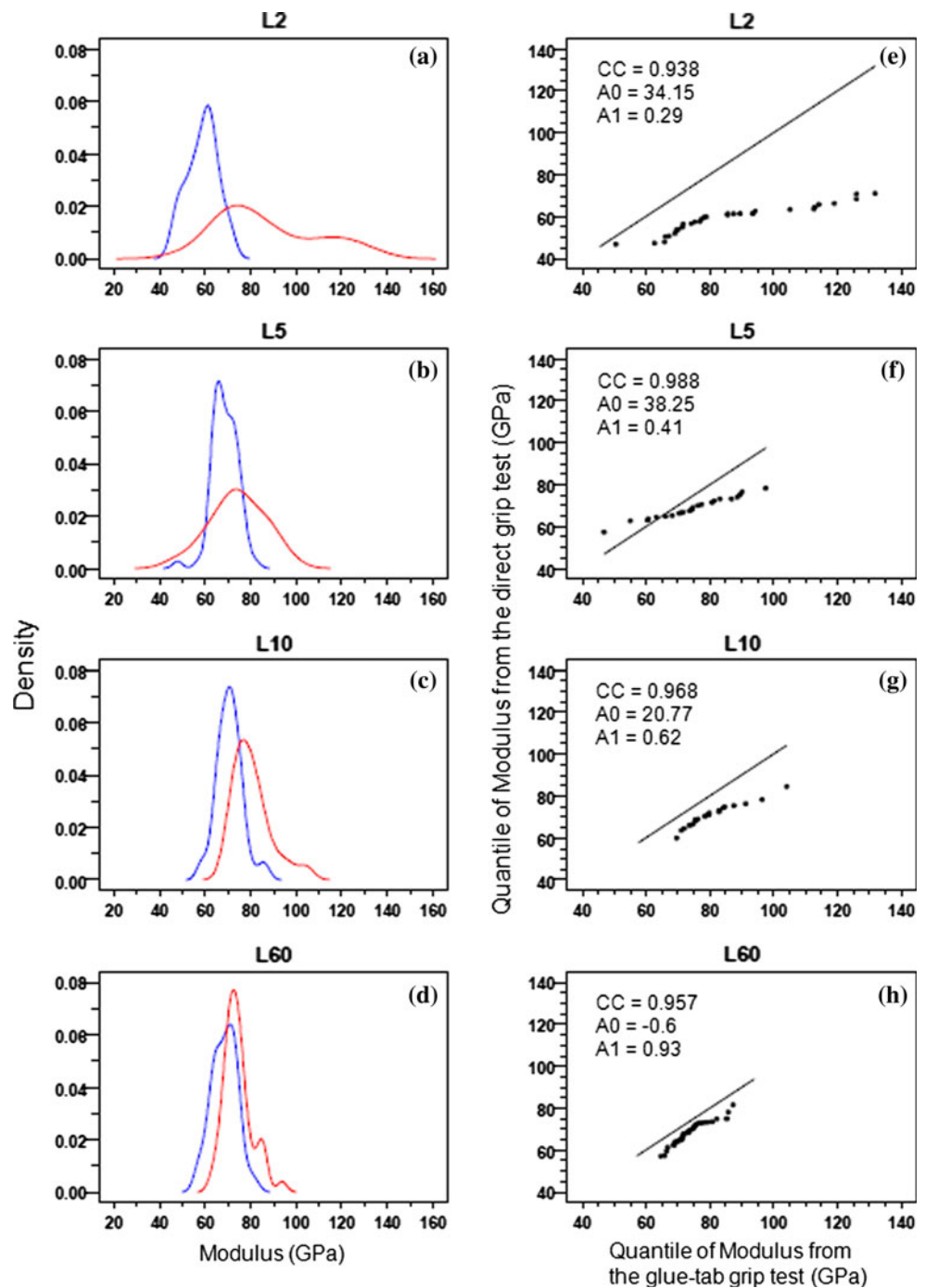Graphical demonstration for statistics of fiber tensile modulus

The kernel density plots (see Fig. 6a–d) of the fiber tensile modulus are shown with the q–q plots (see Fig. 6e–h) to compare and differentiate between the distributions of the modulus data. The kernel density plots of the modulus obtained by the glue-tab grip are significantly broader at

2-mm and somewhat broader at 5-mm fiber lengths compared to the direct grip tests, which corroborate the larger scattering of the data seen in Fig. 3. Although the average modulus of the 2-mm glue-tab tests in Fig. 3 was somewhat higher than 5 mm, the kernel density plot suggests that the apparent higher modulus value is due to the broad second peak at higher modulus values. The higher repeatability of the kernel density plots showing a narrower width for the direct grip test at 2 mm can be attributed to the constant gripping effect and lack of adhesives. Since there is greater influence of the gripping effect as fiber length decreases, the modulus data obtained by longer fiber lengths should be less affected by the gripping effect. Disregarding the data obtained for the 2-mm fiber length, the highest peaks in the density plots are located around 74 GPa within a range of 73–77 GPa for the glue-tab grip tests and 69 GPa within a range of 66–71 GPa for the direct grip tests. These constant trends for both grip tests over the 5-mm fiber length may indicate a negligible gripping effect for the fibers. This suggests that 5 mm is the lowest practical limit of the fiber gauge length to test with the current gripping methods. Figure 6 shows the q–q plots of the modulus data obtained by the glue-tab and direct grip tests. The difference between the two modulus datasets for each gauge length is well demonstrated in the q–q plots graphically, which is indicated by the deviation from the 45° reference line.

Graphical demonstration for statistics of fiber failure strains

The kernel density plots of the fiber failure strains measured by the glue-tab and direct grips are shown in Fig. 7a–d. The kernel density plots of the strains by the glue-tab grip tests also show broader distributions than the direct grip test results for the shorter gauge lengths from 2 to 10 mm. The peaks of the density plots, indicating maximum occurrence of the measured strains, shift to higher strain regions as gauge length decreases in the case of the direct grip, but such a shift is not observed in the glue-tab grip tests, which provides confirmation that the failure strains obtained by the glue-tab grip tests are distributed differently compared to those obtained by the direct grip tests. The q–q plots for the failure strains from the two tests are shown in Fig. 7 displaying deviations from the reference line, which indicate that the strain distributions of the glue-tab grip do not agree with those of the direct grip. Deviations at the shorter gauge lengths with 2, 5, and 10 mm shown in Fig. 7e–g, respectively, are more pronounced than those at 60 mm (Fig. 7h).

Fig. 6 Kernel density plots (**a**, **b**, **c**, **d**) and q–q plots (**e**, **f**, **g**, **h**) for tensile moduli obtained by the glue-tab (*red*) and direct grip (*blue*) tests with 2-mm (**a**, **e**), 5-mm (**b**, **f**), 10-mm (**c**, **g**), and 60-mm (**d**, **h**) fibers (Color figure online)


Graphical demonstration for statistics of fiber tensile strengths

The kernel density plots of the fiber tensile strengths are shown in Fig. 8 for comparison of the glue-tab and direct grip individual strengths calculated using individual diameters. The kernel densities of the glue-tab grip are wider than those for the direct grip, except for the 2-mm case. The peaks of the densities for the direct grip shift to higher strength regions as the fiber length decreases, whereas no significant shift is observed for the glue-tab grip.

The q–q plots of Fig. 8 directly compare quantiles of fiber strengths measured by the glue-tab and direct grips. Deviations from the reference line indicate that the strength distributions of the direct grip do not generally agree with those of the glue-tab grip. It is observed that the quantiles of the strengths measured by direct grip are generally higher than those of the glue-tab grip for 2- and 5-mm gauge lengths as opposed to the longer gauge lengths.
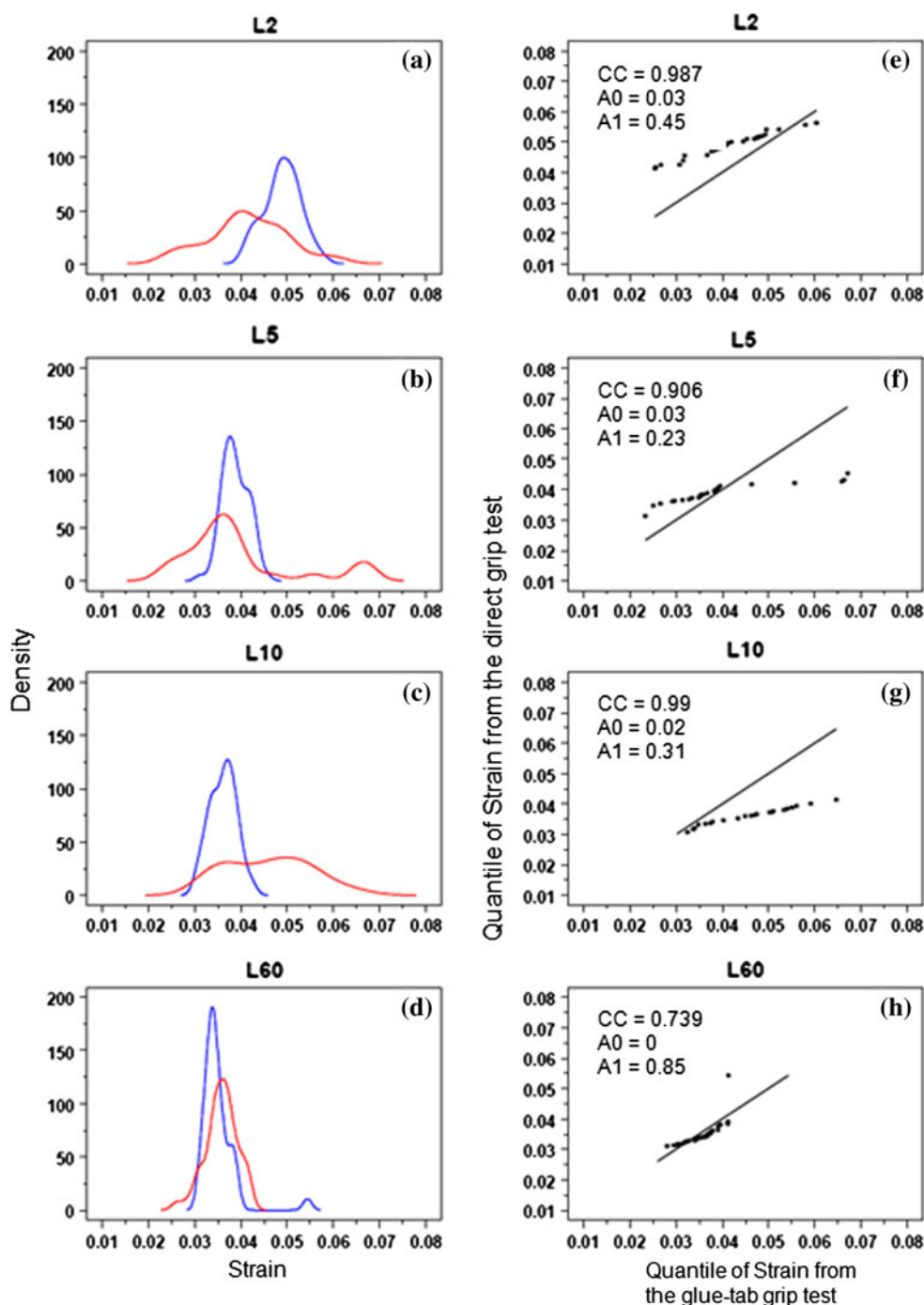
Fig. 7 Kernel density plots (**a**, **b**, **c**, **d**) and q–q plots (**e**, **f**, **g**, **h**) for tensile failure strains obtained by the glue-tab (*red*) and direct grip (*blue*) tests with 2-mm (**a**, **e**), 5-mm (**b**, **f**), 10-mm (**c**, **g**), and 60-mm (**d**, **h**) fibers (Color figure online)

These clear strength dominance patterns of the direct grip in shorter gauge lengths, also visible in the density plots, reconfirm the higher strength values that were measured by the direct grip.

So far, we have compared data tested by two different gripping methods. In general, since many measurements are found to conform to a normal distribution and calculation of strength is a function of the failure load and fiber cross section, these three variables are analyzed here for normality. Table 1 shows the results of one normality check. *P* values exceeding 0.05 are taken to be indicative that the data are compatible with an assumption of normality [19]. *P* values of the load data for both grips indicate conformance to a normal distribution for the failure loads along all fiber lengths. In contrast, the fiber diameters for 60 mm for the glue-tab and 2 and 5 mm for the direct grip

Fig. 8 Kernel density plots (**a**, **b**, **c**, **d**) and q–q plots (**e**, **f**, **g**, **h**) for tensile strengths obtained by the glue-tab (*red*) and direct grip (*blue*) tests with 2-mm (**a**, **e**), 5-mm (**b**, **f**), 10-mm (**c**, **g**), and 60-mm (**d**, **h**) fibers (Color figure online)
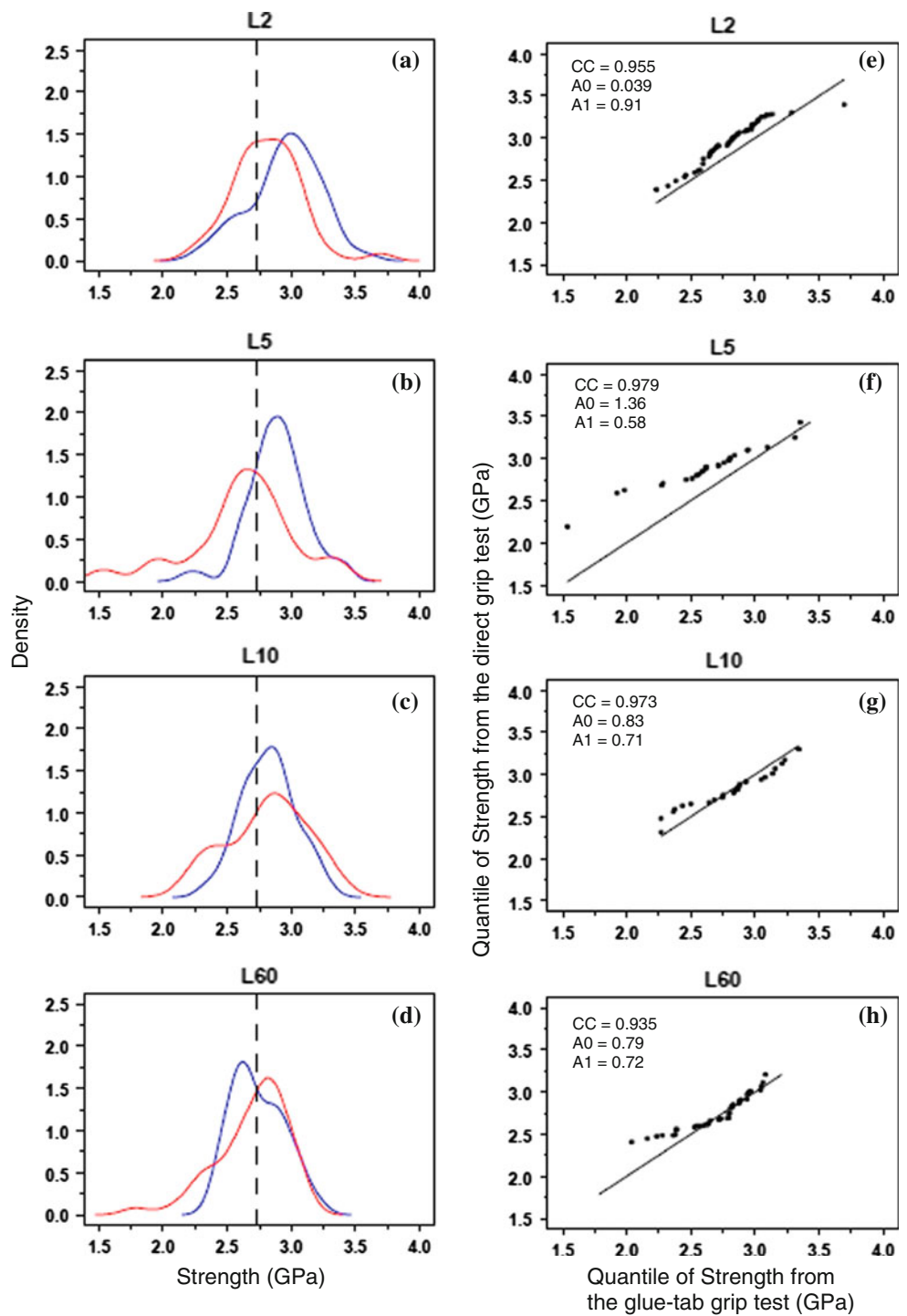
Table 1 Anderson-Darling normality test results for the properties of the fibers (P value < 0.05 indicates non-normal distribution of data)

Gauge length (mm)	P value (the glue-tab grip)			P value (the direct grip)		
	Load	Fiber diameter	Strength	Load	Fiber diameter	Strength
2	0.063	0.310	0.629	0.091	0.001	0.353
5	0.958	0.971	0.158	0.996	0.006	0.277
10	0.992	0.719	0.365	0.473	0.086	0.988
60	0.237	0.011	0.015	0.250	0.450	0.220

are non-normal, and the tensile strength in 60 mm for the glue-tab is not normal.
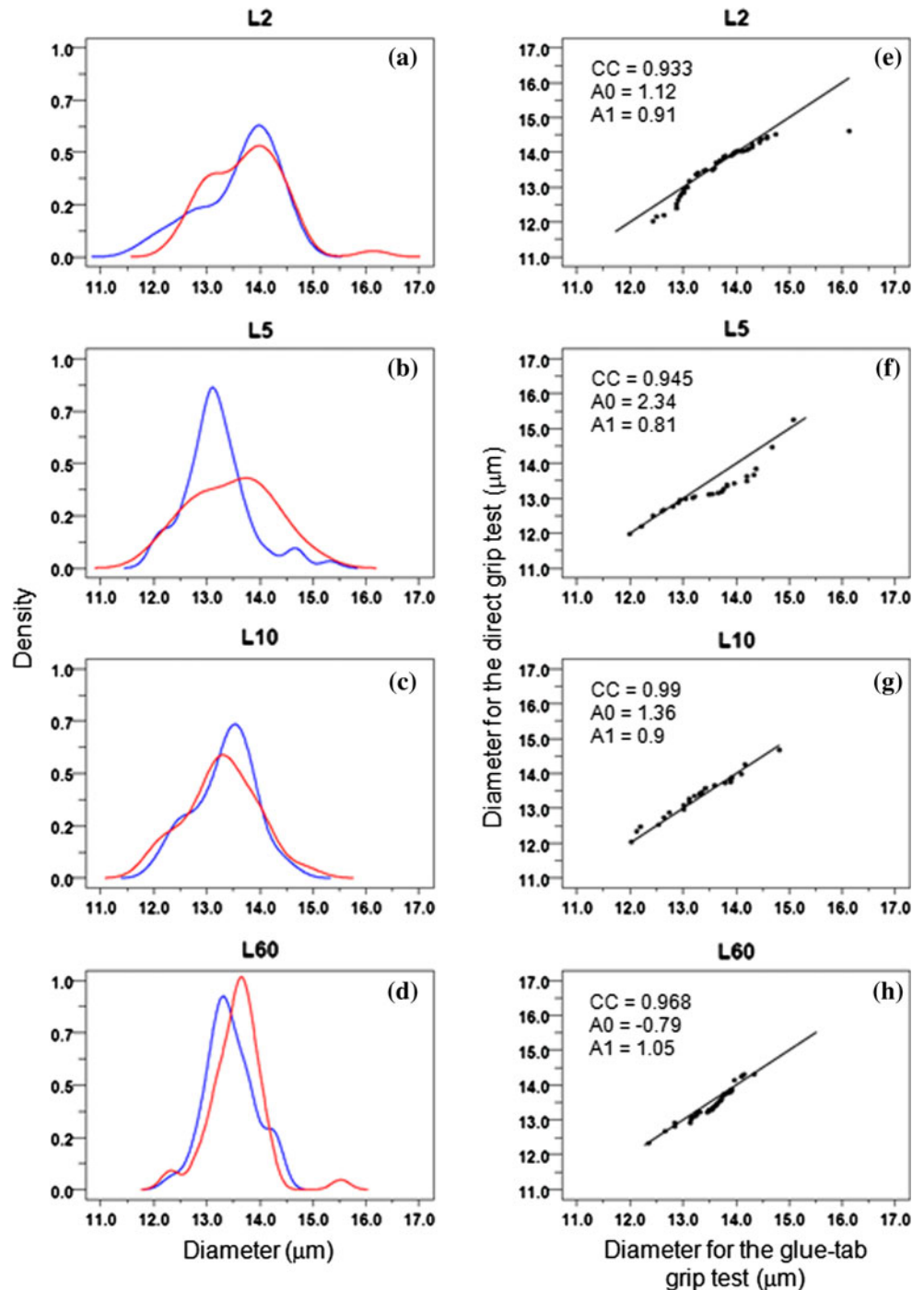
In general, the distribution of the ratio for two variables exhibiting normal distributions is not normal. If the distributions of loads and diameters (i.e., fiber cross-sectional area) are approximately normal, it does not necessarily imply that their ratio (i.e., strength) must also be approximately normal. Therefore, deviation of strength data from normality cannot necessarily be regarded as a measurement
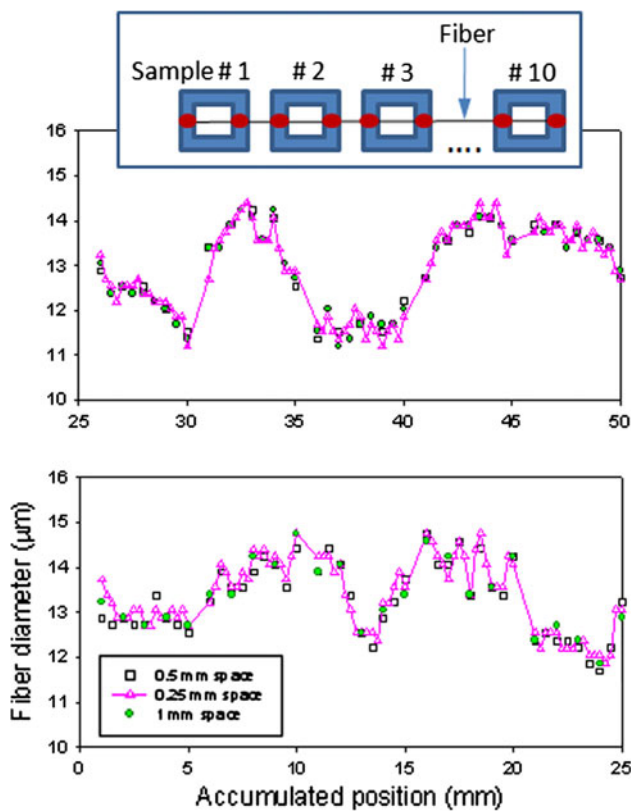
error. One possible reason for the non-normal strength distribution observed will be discussed in the next section.

Variation in fiber diameters and its effect on fiber failure

In the previous section, the tensile strengths were statistically analyzed to investigate gripping effects, and the distribution of the strengths for the 60-mm gauge length of the

Fig. 9 Kernel density plots (**a**, **b**, **c**, **d**) and q–q plots (**e**, **f**, **g**, **h**) for fiber diameters for the glue-tab (*red*) and direct grip (*blue*) tests with 2-mm (**a**, **e**), 5-mm (**b**, **f**), 10-mm (**c**, **g**), and 60-mm (**d**, **h**) fibers (Color figure online)

Fig. 10 Fiber diameter variations of multiple samples fabricated by a single fiber for 5-mm gauge length

with 5 mm is considerably wider than the direct grip, which contributes negatively to the strength calculation. The deviations from 45° reference line of the q–q plots are more significant for the 2- and 5-mm gauge lengths as compared to the 10-mm and 60-mm gauge lengths. Therefore, it is clear that the inhomogeneity of fiber diameters used in this experiment becomes more significant for gauge lengths under the 10-mm length.

This analysis shows that the measured diameter values might be linked to the fiber gauge length. Since the fiber diameter contributes directly to the calculation of strength, variations in diameter can bias strengths where a constant fiber diameter assumption is used. To investigate how fiber diameter measurement can vary based on the measurement scale (i.e., intervals), a single fiber was placed on ten of the 5-mm paper templates to measure diameter as described in the schematic of Fig. 9, equivalent to measuring an approximately 50-mm fiber length. Diameter measurements on the individual specimens were equally spaced at 0.25, 0.5, and 1 mm, these spacings being similar to the actual measurement scales used in this study. The results of such diameter measurements are shown in Fig. 10. Significant variations are observed in fiber diameter along the length for all measurement cases (i.e., 0.25-, 0.5-, and 1-mm spacing), and discrepancies among diameters measured multiple times by different length spaces are relatively smaller than the variation observed in the diameter itself, which indicates a reproducible measurement. Furthermore, localized variation of the fiber diameters occurs and this variation within short lengths (e.g., less than 5 mm) appears to be smaller than that of the whole 50-mm length, which clearly demonstrates why discrepancies among diameters occur between the shorter (i.e., 2 and 5 mm) and longer (i.e., 10 and 60 mm) fibers. Therefore, the discrepancies of the fiber diameters across the different lengths shown in Table 1 are predominantly caused by real variations in the fibers themselves, not by measurement

glue-tab grip exhibited apparent non-normality. Therefore, the distributions of the fiber diameters for various gauge lengths are graphically analyzed in Fig. 9. Empirical distribution between 0.1 and 0.9 probabilities was computed by integrating the kernel density plot. The density plots obtained by the 2- and 5-mm lengths are broader compared to the 10-mm and 60-mm lengths, being approximately 34 % for the glue-tab grip and 24 % for the direct grip tests. Moreover, the peak shape of the glue-tab grip test

Fig. 11 Fiber fracture pattern showing pointy end (a) and fibrillation-like split (b)

error. The influence of the non-normality of the diameters on the fiber strengths therefore is caused by fiber characteristics. To better detect the localized diameter changes seen in Fig. 10, the fiber should be profiled in three-dimensions rather than the two-dimensional profiling done in Fig. 10. However, the authors are unaware of a technique for doing this.

Another question that naturally arises is the implication of non-uniformity of fiber diameter for fiber failure. Is there any preferred failure location such as at the smallest diameter segments along the length? If this were true, determining fiber strength using average fiber diameters should underestimate strength. To verify failure locations, the fracture surfaces of the fibers were investigated.

Fig. 12 Kernel density plots for the tensile strengths calculated by the individual diameters (*red*) and constant diameter (*blue*) for the glue-tab grip (**a, b, c, d**) and the direct grip cases (**e, f, g, h**) (Color figure online)
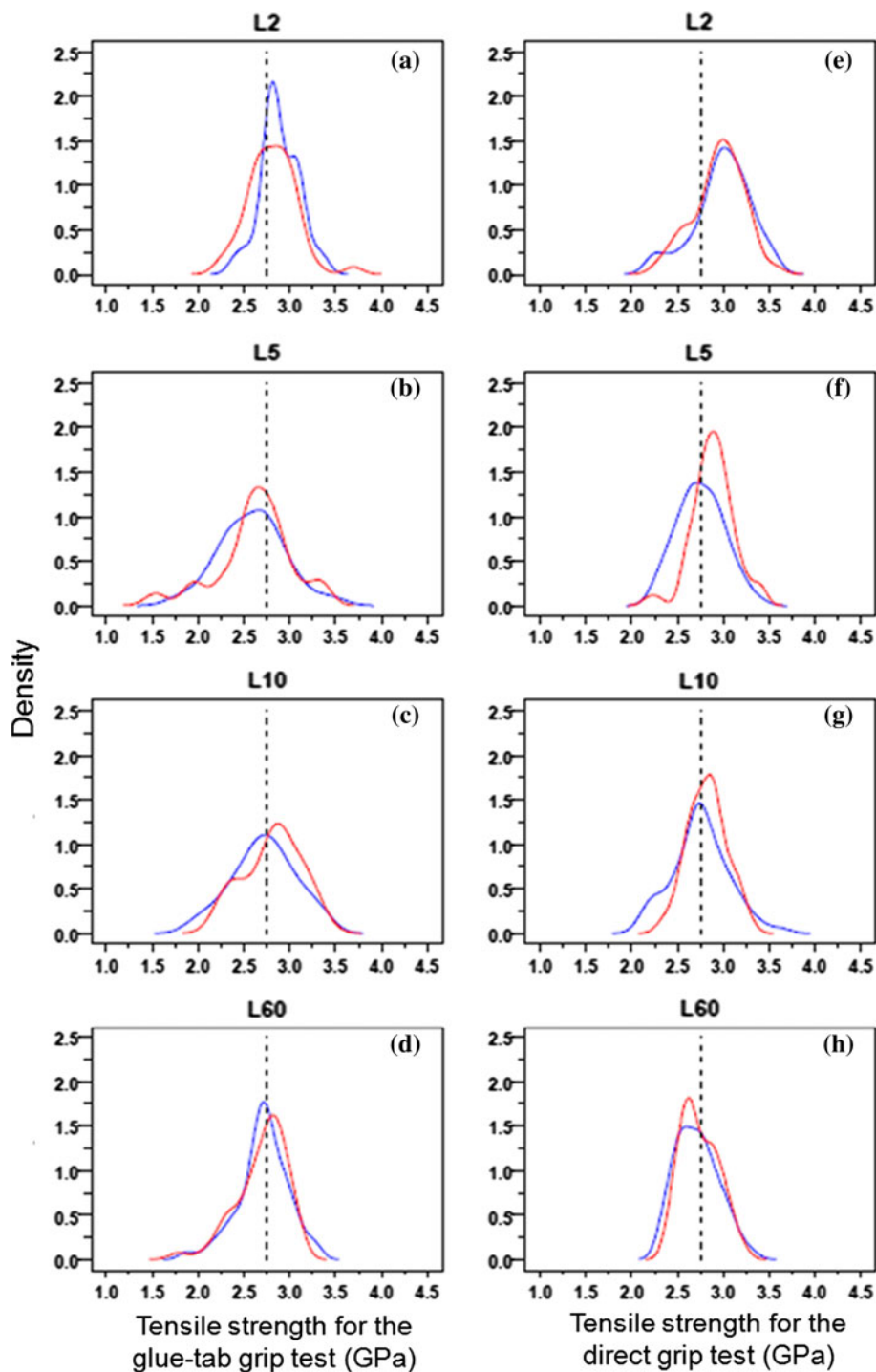
Figure 11 shows a fiber fracture surface after tensile tests. Regardless of the gripping methods, the fracture surfaces of the fiber were either pointy or split ended in a fibrillated manner as shown in Fig. 11a, b. Finding the fracture origin accurately from these kinds of fracture patterns is highly uncertain, in particular with short fiber gauge length because the fracture surface occupies relatively more of the gauge length, and therefore it is hard to assess the relation between the diameter variation and the fracture origin from the fracture surface alone.

Graphical demonstration of the effects of diameter variation on calculating the fiber strength

As briefly described in the previous section, the fiber diameter can be expected to vary along the fiber length, which directly affects strength calculation. If one can assume a true circle for a fiber cross section with negligible variation along the fiber length, an average of multiple distinct diameter measurements (D) can be employed for calculating a strength (F_i, failure load/A, the average fiber

Fig. 13 q–q plots for the tensile strengths calculated by the individual diameters (F_i/A_i) and constant diameter (F_i/A) for the glue-tab grip (**a**, **b**, **c**, **d**) and the direct grip cases (**e**, **f**, **g**, **h**)
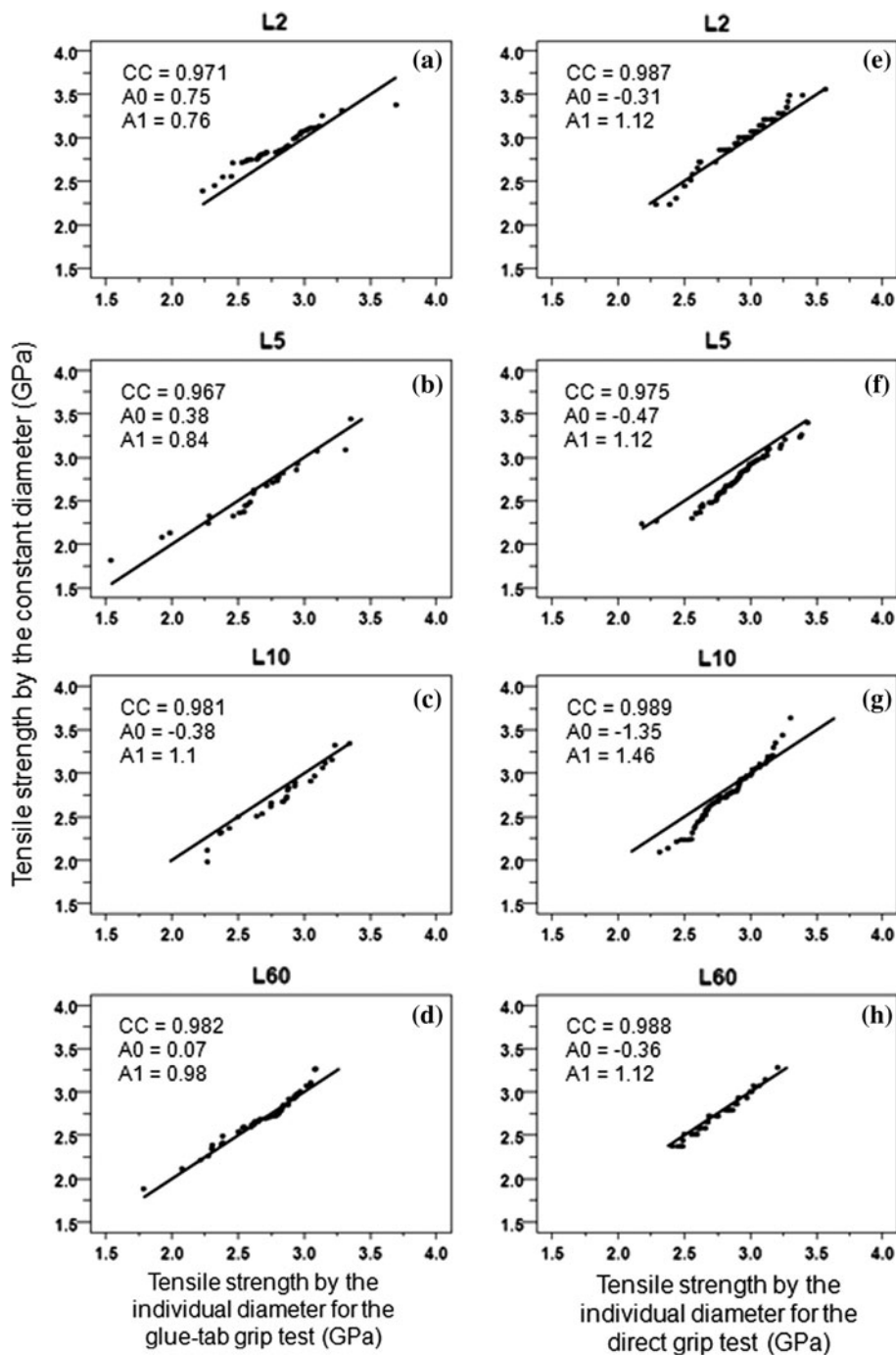
cross-sectional areas ($=\pi D_f^2/4$)) instead of having to estimate and make use of the individual corresponding fiber cross-sectional area ($A_i = \pi D_{f_i}^2/4$) [20], which offers a reduction in test time as an added advantage. However, Monte Carlo simulation to investigate how the strength calculation is influenced by incorporating average fiber diameter versus individual diameters clearly shows the divergence of the two approaches as fiber diameter variation increases; so, individual diameter measurement for true unbiased strength calculation is necessary [21].

To investigate the effect of the fiber diameter variation on strength, the statistics of individual strengths (F_i/A_i) and averaged area strength (F_i/A, $D_f = 13.5$ μm) are shown in Figs. 12 and 13. The kernel density plots of the two cases (F_i/A_i and F_i/A) for the strengths of both grip methods are shown in Fig. 12. The densities of the strengths are somewhat similar at the 60 mm, but appear to be different at 5 and 10 mm for the both grip tests and at 2 mm for the glue-tab grip. Since the broader distributions of the average diameters occur at the short gauge lengths compared to the 60 mm (see Fig. 9), the discrepancies of the density plots for the individual and averaged strengths at the short gauge length are somewhat remarkable.

The differences observed in the kernel density plots are confirmed by the q–q plots in Fig. 13 showing deviations from the 45° reference line with this deviation becoming more significant at the shorter gauge lengths compared to the 60-mm length. Using constant diameter for the individual strength calculation, the fiber strengths are either underestimated (i.e., $L = 10$ for the glue-tab grip, $L = 5$ for the direct grip) or overestimated (i.e., $L = 2$ for both grips) or both ways (i.e., $L = 10$ for the direct grip); thus, strength values depend on the true fiber diameters on each fiber gauge length. These differences become less significant at the 60-mm length for both grips, and this might be caused by the lower probability of using localized fiber diameters for the strength calculation compared to the shorter gauge lengths.

The contrast between approximation for constant diameter assumption and individual diameter measurement can be summarized as follows: If all $A_i \neq A$, then $F_i/A_i \neq F_i/A$ in general. Therefore, it is also usually true that average $[F_i/A_i] \neq$ average $[F_i/A]$, and variance $[F_i/A_i] \neq$ variance $[F_i/A]$. However, for the case where the coefficient of variance of the diameters is sufficiently small, the above inequalities for average and variance of the diameters can become approximate equalities.

Conclusions

In this study, tensile tests were carried out using two different gripping methods to investigate the relative effects

of each on test results. In the direct grip for tensile tests, the fiber was directly gripped, whereas the fiber was glued to a tab for the glue-tab grip tests. Statistical comparisons were conducted graphically to compare the distribution of the mechanical properties of the PPTA fibers as tested by both gripping methods. Compared with the glue-tab grip test exhibiting broader distributions in the kernel density plots particularly in the case of the 2-mm gauge length, the distributions of the tensile moduli obtained by the direct grip test are narrower, which indicates consistent gripping effects over the various fiber lengths. The distributions of the moduli for both tests are similar at the 60-mm gauge length.

The failure strains obtained by the glue-tab grip also show broader distributions compared to the direct grip tests. This difference of the strains between the two tests is smaller at the gauge length 60 mm. The tensile strengths determined by individual failure loads and cross-sectional areas show a similar behavior with the strains over the fiber gauge lengths, but the differences of the distribution sizes for the gripping methods are smaller than the strains. Existence of diameter variations along the fiber for the different gauge lengths used in this work was shown to be characteristic of the fibers themselves.

Since the diameter variation along the fiber gauge length was significant, the density plots of the strengths calculated by the individual diameters did not agree with those calculated using the average diameters. However, this discrepancy for the shorter gauge length disappears at longer gauge lengths. Even though further study is necessary, based on these analyses, the direct grip approach would appear to be more desirable for PPTA fiber tensile tests with short gauge lengths.

References

1. Cheeseman BA, Bogetti TA (2003) Compos Struct 61:161
2. NIST technical workshop on research and metrology of ballistic fibers, Gaithersburg, Maryland, 3–7 October 2007
3. Multi-scale materials behavior in ultra-high loading rate environments, US army research laboratory workshop, APG, Towson, Maryland, 22–23 September 2008
4. Cheng M, Chen WN, Weerasooriya T (2005) J Eng Mater Technol Trans ASME 127:197
5. Tan VBC, Zeng XS, Shim VPW (2008) Int J Impact Eng 35:1303
6. Whitney JM, Daniel IM, Pipes RB (1982) Experimental mechanics of fiber reinforced composite materials, 1st edn, p 151
7. Kim J, McDonough WG, Blair W, Holmes GA (2008) J Appl Polym Sci 108:876
8. Thomason JL, Kalinka G (2001) Compos Part A Appl Sci Manuf 32:85
9. Kobayashi H, McDonough WG, Dunkers JP, Wight SA, Lee HJ, Kim JH, Forster AL, Rice KD, Holmes GA (2012) Polym Compos 33:803

10. Kim JH, Heckert NA, Leigh SD, Kobayashi H, McDonough WG, Rice KD, Holmes GA (2011) In: SAMPE 2011 technical conference proceedings

11. Quantile–Quantile plot in (2003) NIST SEMATECH e-Handbook of statistical methods (http://www.itl.nist.gov/div898/handbook/eda/section3/qqplot.htm)

12. Chambers JM, Cleveland WS, Kleiner B, Tukey PA (1983) Graphical methods for data analysis. Wadsworth International group, Belmont

13. Silverman BW (1982) Appl Stat J Royal Stat Soc Series C 31:93

14. Thomason JL, Kalinka G (2001) Compos Part A Appl Sci Manuf 32:85

15. Fawaz SA, Palazotto AN, Wang CS (1992) Polymer 33:100

16. Horgan CO (1974) Int J Solids Struct 10:837

17. Arridge RGC, Folkes MJ (1976) Polymer 17:495

18. Vanderzwaag S (1989) J Test Evaluation 17:292

19. Schervish MJ (1996) Am Stat 50:203

20. Petry MD, Mah TI, Kerans RJ (1997) J Am Ceram Soc 80:2741

21. Lara-Curzio E, Russ CM (1999) J Mater Sci Lett 18:2041